IOPscience iopscience.iop.org

Home Search Collections Journals About Contact us My IOPscience

Spin-wave-assisted photoluminescence in MnO crystals

This article has been downloaded from IOPscience. Please scroll down to see the full text article.

1990 J. Phys.: Condens. Matter 2 5225

(http://iopscience.iop.org/0953-8984/2/23/013)

View the table of contents for this issue, or go to the journal homepage for more

Download details:
IP Address: 171.66.16.103
The article was downloaded on 11/05/2010 at 05:58

Please note that terms and conditions apply.

J. Phys.: Condens. Matter 2 (1990) 5225–5232. Printed in the UK

Spin-wave-assisted photoluminescence in MnO crystals

Shōsuke Mochizuki†, Bernard Piriou‡ and Jeannette Dexpert-Ghys‡

† Department of Physics, College of Humanities and Sciences, Nihon University, 3-25-40 Sakurajosui, Setagaya-ku, Tokyo 156, Japan

‡ Laboratoire des Elements de Transition dans les Solides, UPR210-CNRS, 1 Place A Briand, 92195 Meudon, France

Received 4 January 1990

Abstract. We report the observation of the photoluminescence in antiferromagnetic and paramagnetic MnO. Two strong emission bands centred at 1.66 and 1.25 eV are observed below the Néel temperature, 118 K, in MnO crystals. Above the Néel temperature, the emission band centred at 1.66 eV vanishes, while the band centred at 1.25 eV persists and remains in the paramagnetic phase at least to room temperature. The photoluminescence is interpreted in terms of a model in which the emissions originate from the impurity-perturbed Mn^{2+} excitons. In the model, the observed emissions arise from the transitions assisted by magnons and the short-wavelength magnetic excitations. The excitation spectra, the time-resolved emission spectra, and the heat-treatment effect on the emission spectra are also reported and discussed.

1. Introduction

In this paper, we report on observations of spin-wave-assisted photoluminescence in MnO in both its antiferromagnetic and paramagnetic phases. The two strong emission bands observed are attributed to the decay of the impurity-perturbed Mn^{2+} excitons accompanied by magnons and the short-wavelength collective excitations.

MnO is a paramagnetic crystal which has a NaCl type crystal structure at room temperature. At 118 K it undergoes a paramagnetic to antiferromagnetic transition that is accompanied by cubic-to-rhombohedral crystallographic distortion. In both the phases, there are several optical absorption bands in the visible and near-ultraviolet regions due to the crystal-field transitions of the Mn^{2+} ions (Huffman *et al* 1969, Yokogawa *et al* 1977, Mochizuki 1988). Although these transitions are strictly forbidden by the spin and parity selection rules, the observed bands have considerable oscillator strengths. In order to interpret these intense absorption bands, various models for the absorption mechanism have been proposed such as: (i) the phonon perturbation model, (ii) the spin-orbit interaction model and (iii) magnon-sideband absorption model (Motizuki and Harada 1970). In model (iii), the long-wavelength magnon breaks the inversion symmetry and causes the electric-dipole magnon sidebands. The magnon sideband absorption arises from the simultaneous creation of a Mn^{2+} exciton and magnon. The existence of the short-range magnetic order in MnO in the temperature range up to about 530 K, has been ascertained very recently by the spin-polarised photoelectron diffraction method (Hermsmeier *et al* 1989). The electronic structure of the transition-metal oxides has long been a controversial topic. Until recently, the generally accepted

0953-8984/90/235225 + 08 $03.50 © 1990 IOP Publishing Ltd

viewpoint was that these oxides are Mott insulators with a large excitation gap due to strong d–d Coulomb correlation effects. Recently, many theoretical models and energy-band calculations have been reported, but they cannot explain the crystal-field absorption and the photoconductivity spectra (Mochizuki 1988). As shown in the studies on the other antiferromagnetic compounds, such as MnF_2 and $MnCO_3$, the photoluminescence spectra offer information on the electronic and the magnetic structures. So far as we know, however, until now no study has been reported on the photoluminescence in MnO. In this paper we report on our investigations of the photoluminescence in MnO.

2. Experimental details

Nominally pure single-crystal boules of MnO were grown by the Verneuil method. Many plates of MnO were obtained by slicing the boules along the cleavage plane and were examined by x-ray analysis, infrared spectroscopy, and microscopy observations. We selected the crystals which did not show the presence of some higher-oxidation states of Mn. The crystals were annealed for 3 h at 1273 K in a 10% H_2–90% Ar atmosphere, which yields fully reduced MnO. The crystals were polished to optical quality.

The specimens were mounted on the cold finger of a metal cryostat or were mounted in a silica glass Dewar and immersed directly in liquid nitrogen. The specimen temperature was measured with a calibrated copper-constantan thermocouple.

The emission spectra were obtained by using an Ar ion laser or a high-pressure mercury arc lamp with a monochromatic system as the excitation source and a monochromator (Jobin–Yvon H-20 IR or Hitachi EPU-2A) with either a germanium detector (North Coast Scientific Corp. EO-817L) or photomultiplier (Hamamatsu R928 and R1477) depending on the wavelength region. The intensity of the exciting beam was kept below 1 mW cm^{-2} to minimise specimen heating and to prevent specimen damage.

The time-resolved emission spectra were obtained as follows. Luminescence was excited by a pulsed dye-laser (Jobin–Yvon LA04/E1T) excited by a N_2 laser and analysed through a double monochromator spectrometer. The information was extracted via a digital oscilloscope (Tektronix 2430) coupled to a 16-bit computer (BFM 187). The time evolution of the emitting level was thus recorded for each pulse. The emitted intensity was be numerically integrated for a chosen gate after a given delay time with respect to the pulse. By programming the data collection as a function of the spectrometer scanning, the time-resolved emission spectra for various integration gates were simultaneously recorded.

The excitation spectra were obtained by using a Xe arc lamp with a monochromatic system (Jobin–Yvon H-20 UV) as the excitation source and the monochromator (Jobin–Yvon H-20 IR) with the germanium detector as the observation system.

In the emission spectra and excitation spectra measurements, the intensity of the excitation beam was modulated by a variable-frequency mechanical chopper and the luminescence signals were measured with a lock-in amplifier (NF LI-570). The spectral response of the optical system including the focusing lenses and mirrors was carefully measured using a calibrated source, and was used to correct the raw data.

3. Results

It is well known that MnO crystals are readily oxidised by air at temperatures only slightly above room temperature and that they are metal-deficient. The deviation from

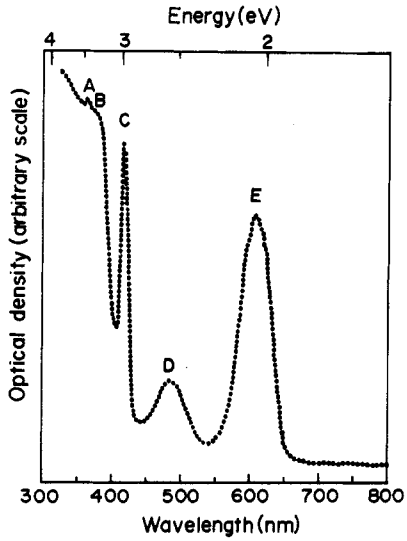

Figure 1. Optical density spectrum at 78 K for the heat-treated MnO crystal.

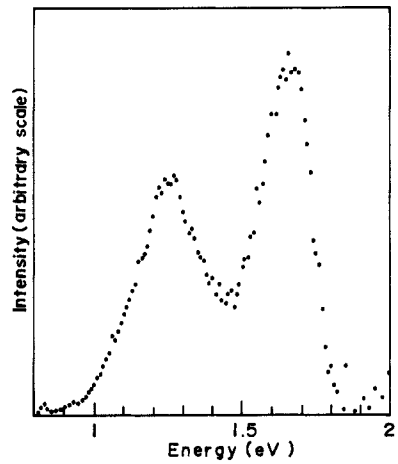

Figure 2. Photoluminescence spectrum at 77 K for the heat-treated MnO crystal. The excitation wavelength is 488.0 nm.

stoichiometry could be sufficient, in many cases, to affect the observed optical properties. Further oxidation leads to the formation of Mn_3O_4 domains on the surface of the MnO crytals and it is known that such MnO crystals with Mn_3O_4 domains can be fully reduced to MnO in a hydrogen gas stream at about 1273 K. In the past, such care has seldom been used in optical studies of MnO. Before the measurements of the photoluminescence, we examined the transmissivity spectra of many MnO crystals before and after the heat-treatment mentioned above. Figure 1 shows the optical density spectrum of the heat-treated MnO crystals with a thickness of 0.2 mm at 78 K. These absorptions of MnO result from transitions from the ground state $^6A_{1g}$ to $^4_aT_{1g}$, $^4_aT_{2g}$, $^4_aA_{1g}$: $^4_aE_g$, $^4_bT_{2g}$ and $^4_bE_g$, which are labelled E, D, C, B and A, respectively in figure 1. Although the absorption band A is not clearly seen in this spectrum, it becomes visible at 356 nm with decreasing specimen thickness. This spectrum is close to those reported by other workers (Huffman *et al* 1969, Yokogawa *et al* 1977, Mochizuki 1988). However, the present measurements on many MnO crystals show the following features: (i) the background absorption in this spectral region can be reduced by the heat-treatment mentioned above, (ii) the intensity ratios between the observed bands are dependent on thermal history of the specimens, and (iii) the peak wavelengths of the observed bands are also specimen-dependent. These features have not been pointed out in previous studies.

We also measured the emission spectra of specimens at 77 K with the 488.0 nm excitation. Two typical spectra of such MnO crystals are shown in figures 2 and 3. Figure 2 shows the spectrum for the heat-treated crystal, while figure 3 shows that for some as-grown crystals. Although the maximum intensities for the two spectra are set to nearly the same value, the emission from the heat-treated crystal is stronger by at least two orders of magnitude than that from the as-grown crystal. The two-band type spectrum, as shown in figure 2, appears in the measurements for the heat-treated crystals and most of the as-grown crystals, but the one-band type spectrum as shown in figure 3 appears in the measurments for a few of the as-grown crystals. It can be seen from these figures

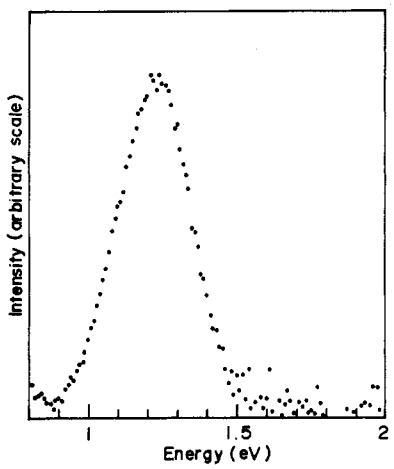

Figure 3. Photoluminescence spectrum at 77 K for some as-grown MnO crystals. The excitation wavelength is 488.0 nm.

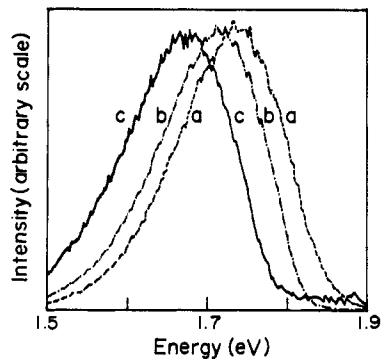

Figure 4. Time-resolved emission spectra at 77 K for the heat-treated MnO crystal. The excitation wavelength is 510.0 nm. Spectra a, b and c correspond to those of the intensities integrated from 0 to 1 μs, from 4 to 18 μs and from 600 to 900 μs after excitation, respectively.

that two broad bands appear at 1.25 and 1.66 eV for the heat-treated crystal and for most of the as-grown crystals, while a broad band only appears at 1.23 eV for the limited as-grown crystals. The Stokes' shifts amount to at least 0.37 eV (3000 cm^{-1}), which are just higher than those of other manganese compounds, MnF_2 (Greene *et al* 1968) and $MnCO_3$ (Komura *et al* 1985).

In order to study the structure of the observed broad emission bands, we measured the time-resolved emission spectra of these crystals at 77 K. Figure 4 shows the spectra obtained for the heat-treated MnO crystal. Spectra a, b and c correspond to those of the intensities integrated from 0 to 1 μs, from 4 to 18 μs and from 600 to 900 μs after excitation, respectively. These are raw spectra, taken without correction for the spectral response of the optical system used. The maximum intensities for the three spectra are set to nearly the same value. The excitation was produced by using the 510.0 nm line emitted from the pulsed dye-laser. As seen in this figure, the decay time increases as the emission energy decreases. This is a typical indication that the emission band centred at 1.66 eV comes from many electronic levels. Fluorescence decays are not exponential; nevertheless one can consider average lifetimes. Their typical values are listed in table 1. Moreover, it is found that the above-mentioned time-resolved spectra does not depend on the excitation energy. It indicates that the observed emissions do not come from the Mn^{2+} exciton bands but from other electronic levels and that the electronic levels (bands) can be populated by the upper Mn^{2+} excited levels. Unfortunately, we could not obtain such information for the emission band centred at 1.25 eV, because we do not have access to a high-speed type near-infrared detector for the time-resolved spectroscopy.

Using the same heat-treated crystal, we studied the excitation spectra at 78 K. Figure 5 shows the excitation spectra of the emission bands centred at 1.25 and 1.66 eV. A comparison of these excitation spectra with the optical density spectrum shown in figure 1 indicates that the excitation efficiency peaks correspond to the crystal-field peaks of Mn^{2+} ions in the cubic field and that the levels in the two emission bands can be populated by the upper-laying Mn^{2+} excited levels, E, D, C, B and A. The energies corresponding

Table 1. Average lifetimes of some levels in the emission band centred at 1.66 eV.

Time elapsed (μs)	Photon energy (eV)		
	1.62	1.71	1.80
0–3	—	—	1
20–60	80	65	50
120–180	140	120	70
600–900	230	205	<100

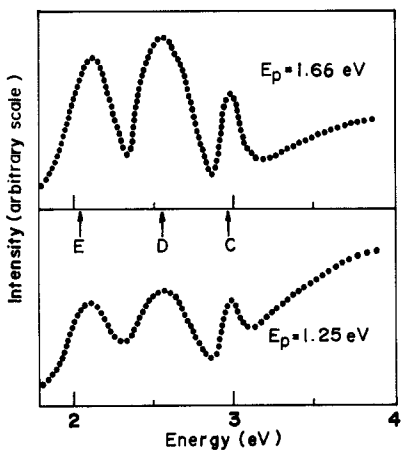

Figure 5. Excitation spectra at 78 K for the heat-treated MnO crystal. The energies E_p = 1.66 and 1.25 eV of the emitted photon energy are the peak energies of the observed emission bands. The energies E, D and C are the peak energies of the absorption.

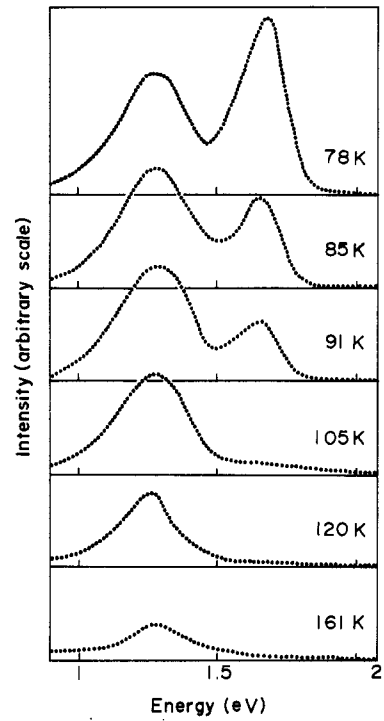

Figure 6. Temperature dependence of the photoluminescence above 78 K for the heat-treated MnO crystal.

to the absorption peaks are indicated by arrows in figure 5. Such comparison also indicates that the emission efficiencies tend to decrease with increasing absorption coefficient. It may arise from some non-radiative transitions induced by surface recombination of the Mn^{2+} excitons. In order to confirm this speculation, we measured the photoluminescence of a nearly stoichiometric MnO powder specimen which was thought to contain more surface-defects than bulk crystal. Certainly, only a very weak emission compared to noise was observed in the powder specimen.

Figure 6 shows the temperature dependence of the emission intensities in the same MnO crystal. As shown in this figure, the emission intensities of both bands decrease with increasing temperature. In particular, above the Néel temperature at 118 K, the

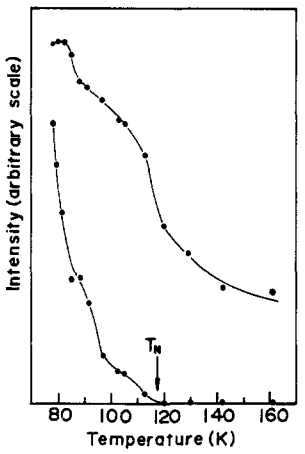

Figure 7. Temperature dependences of the integrated intensity of the emission bands centred at 1.66 and 1.25 eV for the heat-treated MnO crystal. The Néel temperature T_N is indicated by an arrow. Upper and lower curves correspond to the integrated intensities of the band centred at 1.25 and 1.66 eV, respectively.

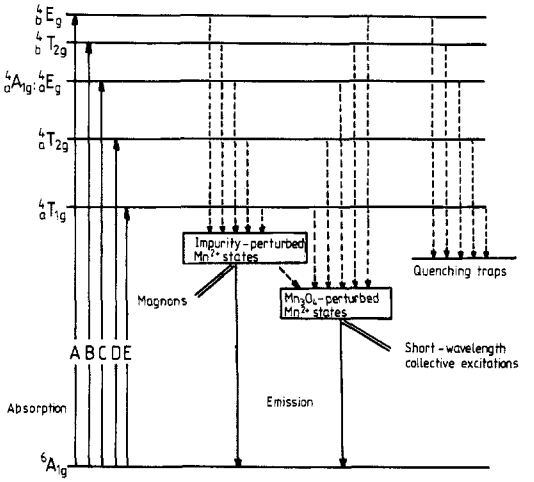

Figure 8. Electron energy scheme for the photoluminescence in MnO crystals. Upward solid arrows indicate the absorptions, downward solid arrows indicate the radiative transitions, downward broken arrows indicate the non-radiative transitions and parallel lines indicate the interactions.

band centred at 1.66 eV disappears in accordance with the vanishing of the long-range magnetic order, while the band centred at 1.25 eV persists in the paramagnetic phase above 118 K, although a conspicuous drop in the emission intensity is observed at 118 K. This temperature behaviour is similar to that observed in the inelastic light scattering in NiF_2 crystals (Fleury 1969) as follows. The one-magnon scattering peak vanishes above the Néel temperature T_N, but the two-magnon peak persists and remains well defined to temperatures of at least 1.5 T_N, indicating the existence of underdamped spin waves in the paramagnetic phase. Although the observed emission bands come from many electronic levels, we tried to reduce the spectra to two bands by assuming that the band centred at 1.25 eV is quasi-symmetrical. The integrated intensities of the two bands obtained are plotted as a function of temperature in figure 7. In the figure, upper and lower curves correspond to the integrated intensities of the band centred at 1.25 and 1.66 eV, respectively. Full curves are added between the points as a guide to show the behaviours.

4. Discussion

The present experimental results on the photoluminescence in MnO may be summarised as follows.

(i) The photoexcitations from the sextet ground state to the quartet excited states of Mn^{2+} ion in MnO crystal induce two broad-band-emissions at 1.66 and 1.25 eV with large Stokes' shifts. The emission spectrum and the emission intensity are very sensitive to the deviation from the stoichiometric composition.

(ii) Except for their intensities the observed emission spectra do not depend on the excitation photon energy.

(iii) The decay times of the luminescences increase with increasing time elapsed and with decreasing emission energy.

(iv) Above the Néel temperature of 118 K, the emission band centred at 1.66 eV disappears, while the emission band centred at 1.25 eV persists and remains in the paramagnetic phase at least to room temperature, though a conspicuous drop of the emission intensity is observed at the Néel temperature.

Point (iv) clearly suggests that the luminescent centres are closely related to the magnetic ordering of the manganese spins in the MnO crystals.

Now let us consider the mechanism of the luminescence in MnO. Using other manganese compounds, MnF_2, $MnCO_3$ and alkali manganese trifluorides, many workers (Greene *et al* 1968, Komura *et al* 1985, Holloway *et al* 1965) have studied similar photoluminescence spectra. In order to explain the observed results, they proposed several models. Holloway *et al* (1965) attributed the extraordinarily large separation between the broad absorption and the emission band peaks to a Stokes' shift which is dependent on the magneto-elastic coupling. On the other hand, Greene *et al* (1968) and Komura *et al* (1985) interpreted such results as an emission composed of multimagnon and multimagnon–phonon sidebands associated with a pure electronic transition between $^6A_{1g}$ and $^4T_{1g}$ states of the manganese ions. Generally speaking, the optical absorptions of antiferromagnetic manganese compounds are accompanied by the creation of Mn^{2+} excitons and by the creation and destruction of magnons. The created excited-states are then destroyed by the creation of photons and by the creation and destruction of magnons, thereby conserving the energy and the momentum. In the present discussion, it is important to know the temperature dependence of the spin-order of MnO above and below the Néel temperature. Recently, Hermsmeier *et al* (1989) have produced evidence for a high-temperature short-range magnetic order transition in MnO at 530 ± 20 K that is 4.5 times the Néel temperature 118 K, by the spin-polarised photoelectron diffraction method. This indicates that the short-range magnetic order persists well into the paramagnetic phase in MnO. In the study of the inelastic light scattering in NiF_2, Fleury (1969) has also indicated that the short-range magnetic order persists well into the paramagnetic phase and also that the short-wavelength magnetic excitations of the paramagnetic phase are relatively long-lived and represent a continuous evolution from what were magnons in the antiferromagnetic phase. To clarify such short-wavelength magnetic excitations (so-called paramagnons or sloppy spin waves) is of vital importance to many workers in the magnetism. In such antiferromagnetic insulators, it may be possible to observe the photoluminescences assisted by both magnons and the short-wavelength magnetic excitations below the Néel temperature, and to observe the photoluminescence assisted only by the short-wavelength magnetic excitations above the Néel temperature. Thus, the results of the temperature dependences of the emission intensities shown in figures 6 and 7 appear to indicate that the emission band centred at 1.66 eV arises from transitions assisted by magnons, while the emission band centred at 1.25 eV arises from transitions by the short-wavelength magnetic excitations. Some attempts have been made to explain the photoluminescences in other manganese compounds, by assuming the existence of the impurity-perturbed Mn^{2+} states or by using the configuration coordinate curves affected by the degree of the spin alignment. However, it is not easy to confirm the validity of these assumptions by experimental methods. By noting the non-stoichiometric nature of MnO crystals, we propose the electronic energy scheme for the photoluminescence in MnO as shown in figure 8. As illustrated in this figure, the optical absorptions produce

the quartet excited states of Mn^{2+} ions and the intrinsic Mn^{2+} excitons. The excitons then decay after a certain time by the following non-radiative processes; (i) the transition to quenching trap levels, (ii) the transition to certain impurity-perturbed Mn^{2+} states, and (iii) the transition to other impurity-perturbed Mn^{2+} states. The impurity-perturbed Mn^{2+} states may come from the Mn^{2+} ion surrounded by impurities or crystalline defects (Mn_3O_4 clusters). In this model, the majority of the Mn^{2+} ions might not be perturbed. Since we cannot detect the intrinsic emission from such unperturbed Mn^{2+} states, this will not be dealt with here. In this case, the excited energy levels of these perturbed Mn^{2+} ions can be shifted to the lower-energy side, thereby creating traps for the freely propagating intrinsic Mn^{2+} excitons. Since the manner of the perturbation is varied, the excited energy levels of the perturbed Mn^{2+} ions produce bands. Then, the luminescent transitions from these bands to the ground state are achieved by the creation and destruction of magnons and the short-wavelength magnetic excitations so as to conserve the energy and the momentum. The type of perturbation may be ascertained by the time-resolved emission spectra in figure 4. Moreover, since, as seen from figures 2 and 3, the emission band centred at 1.66 eV disappears and the only emission band centred at about 1.23 eV persists in some as-grown crystal, the higher-energy band in figure 8 is attributed to the Mn^{2+} states perturbed by certain impurities, while the lower-energy band in figure 8 is attributed to the Mn^{2+} states perturbed by Mn_3O_4 clusters. The heat-treatment enhanced luminescence and point (iii) might indicate that some relaxation processes from higher-energy states to lower-energy states or those from a higher-energy band to a lower energy band are possible. By using this electronic energy scheme, the obtained results shown in figures 1–7 are explained. It should be noted that the temperature dependences of the integrated intensities shown in figure 7 and of the emission spectra shown in figure 6 are similar to the results (figures 1 and 2 in Fleury's (1969) paper) of the inelastic light scattering in NiF_2. These results can be explained by introducing processes assisted by magnons and by the short-wavelength collective excitations.

Acknowledgments

This work was partially supported by the Fund for Science Promotion of Nihon University. This work was also supported by the Joint Studies Program (1989–1990) of the Institute for Molecular Science. We should like to thank Dr K Murayama and Mr T Yamanaka for their assistance in the preliminary measurements of photoluminescence.

References

Fleury P A 1969 *Phys. Rev.* **180** 591
Greene R L, Sell D D, Feigelson R S, Imubusch G F and Guggenheim H J 1968 *Phys. Rev.* **171** 600
Hermsmeier B, Osterwalder J, Friedman D J and Fadley C S 1989 *Phys. Rev. Lett.* **62** 478
Holloway W W, Prohofsky E W and Kestigian M 1965 *Phys. Rev.* **139** A954
Huffman D R, Wild R L and Shinmei M 1969 *J. Chem. Phys.* **50** 4092
Komura H, Fujima N, Yamaguchi T and Ishikawa K 1985 *J. Appl. Phys.* **58** 902
Mochizuki S 1988 *J. Phys. C: Solid State Phys.* **21** 5183
Motizuki K and Harada O 1970 *Prog. Theor. Phys. Suppl.* **46** 40
Yokogawa M, Taniguchi K and Hamaguchi C 1977 *J. Phys. Soc. Japan* **42** 591